

Synthesis, DNA-binding, Photocleavage and *in vitro* Cytotoxicity of Novel Imidazole[4,5-f][1,10]phenanthroline-based Oxovanadium Complexes

Peng Ying¹, Xuyan Tian², Pengfei Zeng¹, Jiazheng Lu^{1*}, Hongyuan Chen^{2*} and Manshan Xiao²

¹Department of Chemistry, School of Pharmacy, Guangdong Pharmaceutical University, Guangzhou, 510006, P.R. China

²Department of Pathogen Biology and Immunology, School of Basic Course, Guangdong Pharmaceutical University, Guangzhou 510060, P.R. China

Abstract

Three novel imidazole[4,5-f][1,10]phenanthroline-based oxovanadium complexes [VO(hntdtsc)(HPIP)] (1) (hntdtsc = 2-hydroxyl-1-naphthaldehyde thiosemicarbazone, HPIP = 2-(2-hydroxyphenyl)imidazole[4,5-f][1,10]phenanthroline), [VO(hntdtsc)(m-HPIP)] (2) (m-HPIP = 2-(3-hydroxyphenyl)imidazole[4,5-f][1,10]phenanthroline), [VO(hntdtsc)(p-HPIP)] (3) (p-HPIP = 2-(4-hydroxyphenyl)imidazole[4,5-f][1,10]phenanthroline), have been synthesized and characterized by elemental analyses and spectroscopic techniques. Their DNA-binding properties with calf-thymus DNA (CT-DNA) were studied by various methods. The cytotoxicity of these three complexes was evaluated by 3-(4,5-dimethylthiazol-2-yl)-2,5-diphenyltetrazolium bromide (MTT) assay. The electronic spectral results reveal that three complexes can bind to CT-DNA by intercalation mode. The electrophoresis studies also show that they can efficiently cleave pBR322 DNA. The *in vitro* antiproliferative activity of complex 1 against human CaSki, SiHa, K562, HepG2, EC9706 and EC109 cell lines is proved to be more effective than both 2 and 3.

Keywords: Oxovanadium complexes; DNA-binding; Photocleavage; Cytotoxicity

Introduction

In recent years, more and more biochemists and pharmacologists have paid their attention to research on other transition metal complexes such as ruthenium (II), copper (II), zinc (II), nickel (II), cobalt (II) complexes compared with traditional platinum compounds in treatment of human cancer due to their potential applications as chemical and stereoselective probes of nucleic acid structures as well as diverse biological activities [1-5]. As a trace bioelement existing in the human body, vanadium has been found to present a variety of physiological activities such as nutritional metabolism [6], insulin mimetic effect [7], as well as closely connected with cell apoptosis and cancer [8]. In the past decades, oxovanadium compounds have been extensively studied for their potential biological and pharmacological activities such as antibacterial [9], biocatalytic oxidation [10], insulin-enhancing effects [11], apoptosis-inducing activity [12], potential capabilities as DNA structural probes and DNA dependent electron transfer likewise [13].

In addition, thiosemicarbazones were often chosen as primary ligands for vanadium owing to their wide range of physiological and pharmacological activities including antifungal [14], antitumor [15], antibacterial [16] and antiviral activities [17]. Oxovanadium complexes incorporated with thiosemicarbazones have demonstrated both *in vitro* antibacterial and antiproliferative properties [18-19] as well as intense interaction with DNA [20]. On the other hand, 1,10-phenanthroline and its derivatives were usually served as a very efficient class of ligands, which lead to efficient catalysis in cross coupling reaction of aliphatic alcohols and aryl halides [21], antimicrobial activities [22], efficient DNA-binding and DNA cleavage [23] thus inducing significant cytotoxicity in the cultured cells [24]. Subsequently, research on mixed-ligand metal complexes has been put into practice in order to combine the pharmacological properties of both the ligands and metal thus reduce toxicity simultaneously [25]. So far, a certain attentions have been paid to Ru (II), Cu (II), Co (II) and Ni (II) complexes incorporating imidazole[4,5-f][1,10]phenanthroline derivatives ligands [26-27]. However, there have been relatively few studies on oxovanadium complexes with imidazole derivatives of 1,10-phenanthroline and their mechanism.

Previously, we have reported some oxovanadium (IV) complexes

incorporating 1,10-phenanthroline (phen) or bipyridyl (bpy) present high DNA intercalator, photocleavage properties and cytotoxicity *in vitro* [13,19-20]. Although the molecular basis for the DNA-binding properties of oxovanadium (IV) compound is not completely understood at the present time, it occurs to us that oxovanadium complexes bearing phen moiety possess higher DNA-binding activities and more potent inhibitory effect against cancer cell lines than that of bearing bpy moiety. The previous results provide strong evidence for us to assume that DNA-binding activity of oxovanadium complexes may increase owing to the introduction of larger aromatic ring in auxiliary ligands substituted with 1, 10-phenanthroline.

In the present work, we have synthesized three unsymmetrical imidazole[4,5-f][1,10]phenanthroline-based oxovanadium complexes [VO(hntdtsc)(HPIP)] (1) (hntdtsc = 2-hydroxyl-1-naphthaldehyde thiosemicarbazone, HPIP = 2-(2-hydroxyphenyl)imidazole[4,5-f][1,10]phenanthroline), [VO(hntdtsc)(m-HPIP)] (2) (m-HPIP = 2-(3-hydroxyphenyl)imidazole[4,5-f][1,10]phenanthroline), [VO(hntdtsc)(p-HPIP)] (3) (p-HPIP = 2-(4-hydroxyphenyl)imidazole[4,5-f][1,10]phenanthroline), and characterized by elemental analysis, IR, molar conductance, ES-MS and ¹H NMR. The DNA-binding properties of these three complexes were well studied by UV-Vis titration, fluorescence spectra, viscosity measurements and thermal denaturation studies. Photocleavage reactions with pBR322 supercoiled plasmid DNA were investigated by agarose gel electrophoresis experiments. Their cytotoxicity *in vitro* against cervical cancer CaSki and SiHa, leukemia K562, HepG2, esophagus carcinoma EC9706 and EC109 cell lines were

***Corresponding authors:** Jiazheng Lu, Department of Chemistry, School of Pharmacy, Guangdong Pharmaceutical University, Guangzhou, 510006, P.R. China, Tel: +86-20-39352122; Fax: +86-20-39352129; E-mail: lujia6812@163.com

Hongyuan Chen, Department of Pathogen Biology and Immunology, School of Basic Course, Guangdong Pharmaceutical University, Guangzhou 510060, P.R. China, Tel: 86-020-3935219; E-mail: hychen1208@126.com

Received June 28, 2014; Accepted July 28, 2014; Published July 31, 2014

Citation: Ying P, Tian X, Zeng P, Lu J, Chen H, et al. (2014) Synthesis, DNA-binding, Photocleavage and *in vitro* Cytotoxicity of Novel Imidazole[4,5-f][1,10]phenanthroline-based Oxovanadium Complexes. Med chem 4: 549-557. doi:10.4172/2161-0444.1000193

Copyright: © 2014 Ying P, et al. This is an open-access article distributed under the terms of the Creative Commons Attribution License, which permits unrestricted use, distribution, and reproduction in any medium, provided the original author and source are credited.

assessed by MTT assay. The compounds employed in this work are shown in Scheme 1.

Experimental

Materials and methods

All starting chemicals used in the synthesis and physical measurements were commercially available reagents and without further purification unless otherwise specified. 1,10-phenanthroline (phen) was obtained from Guangzhou Chemical Reagent Factory. VO(acac)₂ were purchased from Alfa Aesar, thiosemicarbazide (TSC) was purchased from TCI, CT-DNA and pBR322 supercoiled plasmid DNA were obtained from Sigma. Cell lines of CaSki, SiHa, K562, HepG2, EC9706 and EC109 were purchased from American Type Culture Collection. Tris buffer A (Tris=tris(hydroxymethyl) aminomethane) containing 5 mM Tris-HCl and 50 mM NaCl (pH=7.2) was used for absorption titration and viscosity measurements. Tris buffer B containing 50 mM Tris-HCl and 18 mM NaCl (pH=7.2) was used for the gel electrophoresis experiments. Buffer C containing 1.5 mM Na₂HPO₄, 0.5 mM NaH₂PO₄ and 0.25 mM Na₂H₂EDTA (H₄EDTA=N,N'-ethane-1,2-diylbis[N-(carboxymethyl) glycine]) (pH=7.0) was used for thermal denaturation. A solution of CT-DNA in buffer A gave a ratio of UV absorbance at 260 and 280 nm of 1.8-1.9:1, indicating that the DNA was sufficiently free of protein [13,19]. The DNA concentration per nucleotide was determined by absorption spectroscopy using the molar absorption coefficient (6600 M⁻¹ cm⁻¹) at 260 nm [20]. The oxovanadium complexes were dissolved in DMSO and diluted with buffer solution to the required concentrations prior to use. 2-hydroxyl-1-naphthaldehyde thiosemicarbazone (hntdtsc) was prepared according to a previously reported procedure [28].

Physical measurements

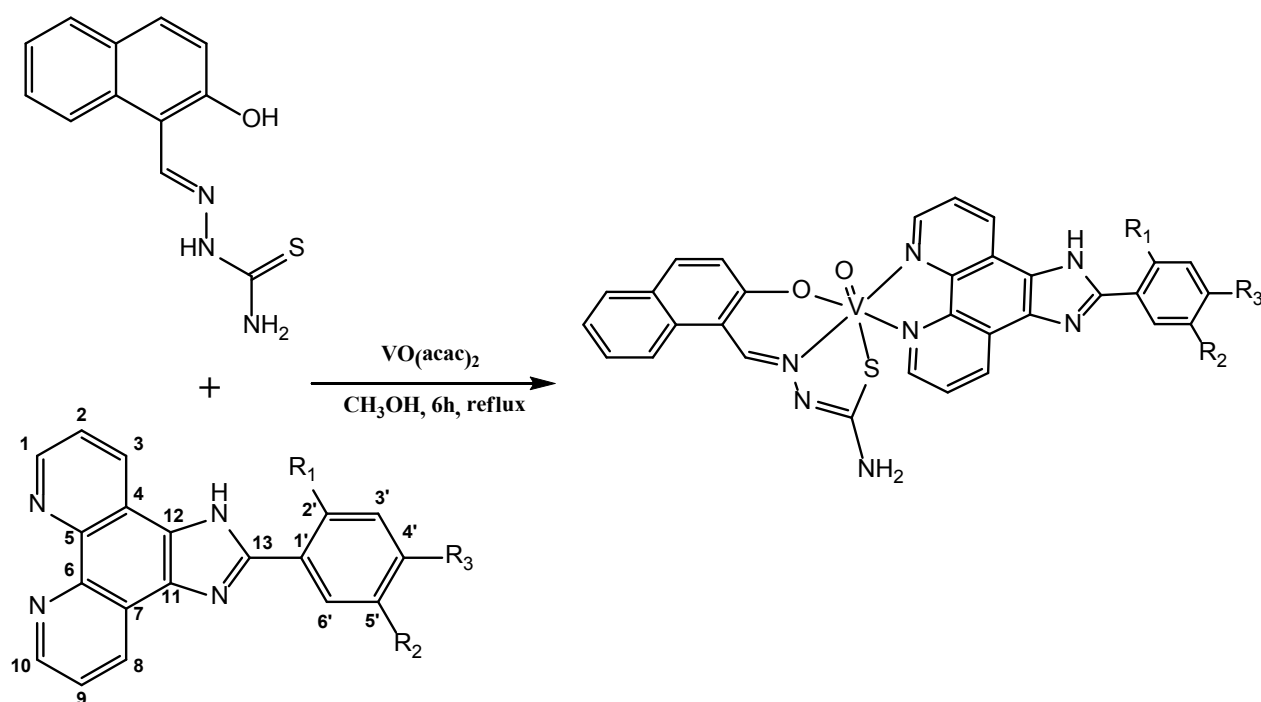
Microanalysis (C, H, and N) was carried out with a PerkinElmer 240Q elemental analyzer. Electrospray mass spectra (ES-MS) were recorded on an LCQ system (Finnigan MAT, USA) using methanol

as mobile phase. ¹H NMR spectra were recorded on a Varian-500 spectrometer. All chemical shifts are given relative to tetramethylsilane (TMS). Infrared spectra were recorded on a Bomem FTIR model MB102 instrument using KBr pellets method. UV-Vis spectra were recorded on a Shimadzu UV-3101 PC spectrophotometer at room temperature. Emission spectra were recorded on a Perkin-Elmer Lambda 55 spectrofluorophotometer. Molar conductivities in DMF (10⁻³M) solution at room temperature were measured using a DDS-307 digital direct reading conductivity meter.

Synthesis of phenanthroline-based ligands: HPIP, *m*-HPIP and *p*-HPIP

HPIP was synthesized through modification of a previously reported method [29]. A mixture of salicylaldehyde (0.69 mL, 5 mmol) and ammonium acetate (7.70 g, 0.1 mol) was added into a stirring solution of 1, 10-phenanthroline-5, 6-dione (0.99 g, 5 mmol) in 60 mL of glacial acetic acid, and the mixture was continuously stirred at 60°C for 6 hours. Then the deep red solution was cooled to room temperature and diluted with 100 mL distilled water. A grayish precipitate was obtained by neutralization with ammonium hydroxide. Then the mixture was filtered and washed with water for three times. The crude solid power was purified by chromatography over 60-80 mesh SiO₂ using absolute ethanol as eluent. The solvent was removed and the products were collected, and dried *in vacuo*. *m*-HPIP and *p*-HPIP were prepared by a similar procedure as for the compound HPIP, with 3-Hydroxybenzaldehyde (0.69 mL, 5 mmol) and 4-Hydroxybenzaldehyde (0.69 mL, 5 mmol) in place of salicylaldehyde (0.69 mL, 5 mmol) respectively, and a grey-white precipitate were obtained.

HPIP: Yield: 86%. Anal. Found: C, 73.12; H, 3.79; N, 18.03; Calcd for C₁₉H₁₂N₄O: C, 73.07; H, 3.87; N, 17.94. ¹H NMR (DMSO-*d*₆, 500 MHz) δ: 12.85 (s, 1H, -NH), 10.07 (s, 1H, -OH), 9.91 (d, 2H, *J* = 7.4Hz, ArH), 9.85 (d, 2H, *J* = 8.0Hz, ArH), 9.28 (d, 1H, *J* = 7.7Hz, ArH), 8.75-



Scheme 1: Synthesis of VO(hntdtsc)(HPIP) (1), R₁=OH, R₂=H, R₃=H; VO(hntdtsc)(*m*-HPIP) (2), R₁=H, R₂=OH, R₃=H; VO(hntdtsc)(*p*-HPIP) (3), R₁=H, R₂=H, R₃=OH.

8.68 (m, 2H, $J = 8.1$ Hz, ArH), 8.23 (t, $J = 7.6$ Hz, 1H, ArH), 7.99-7.90 (m, 2H, $J = 8.3$ Hz, ArH). ^{13}C NMR (DMSO- d_6 , 500 MHz) δ : 157.5 C(2'), 146.4 C(13), 142.9 C(1, 10), 129.6 C(5, 6), 128.6 C(4, 7), 126.2 C(3, 8), 122.9 C(4', 6'), 122.5 C(4, 12), 120.8 C(5'), 118.4 C(2, 9), 116.6 C(1'), 116.3 C(3'). ES-MS: (CH₃OH): m/z 313.0 ([M + H]⁺). IR (KBr disk): ν (cm⁻¹) = 3383.0 (s, $\nu_{\text{O-H}}$), 3255.6 (s), 3264.3 (s, -NH₂), 3186.8 (s, $\nu_{\text{N-H}}$), 3036.8 (m, $\nu_{\text{C-H}}$), 1608.5 (s), 1566.0 (s), 1486.8 (vs, $\nu_{\text{C=C}}$), 738.0 (vs), 699.1 (s, $\delta_{\text{C-H}}$). Conductance ($\Omega^{-1}\text{cm}^2\text{mol}^{-1}$): 8.6.

m-HPIP: Yield: 79%. Anal. Found: C, 73.02; H, 3.67; N, 18.04; Calcd for C₁₉H₁₂N₄O: C, 73.07; H, 3.87; N, 17.94. ^1H NMR (DMSO- d_6 , 500 MHz) δ : 13.52 (s, 1H, -NH), 10.04 (s, 1H, -OH), 9.01 (d, 2H, $J = 7.2$ Hz, ArH), 8.90 (dd, 2H, $J = 8.1$ Hz, 1.5 Hz, ArH), 8.73 (d, 1H, $J = 8.8$ Hz, ArH), 8.12 (d, 2H, $J = 8.6$ Hz, ArH), 7.82 (s, 1H, ArH), 6.99-6.98 (d, 2H, $J = 8.6$ Hz, ArH). ^{13}C NMR (DMSO- d_6 , 500 MHz) δ : 158.9 C(2'), 151.2 C(13), 147.4 C(1, 10), 129.3 C(5, 6), 127.9 C(4, 7), 123.0 C(3, 8), 122.6 C(4', 6'), 122.1 C(4, 12), 120.5 C(5'), 118.8 C(2, 9), 116.7 C(1'), 115.8 C(3'). ES-MS: (CH₃OH): m/z 313.0 ([M + H]⁺). IR (KBr disk): ν (cm⁻¹) = 3383.6 (s, $\nu_{\text{O-H}}$), 3263.0 (s), 3256.5 (s, -NH₂), 3187.0 (s, $\nu_{\text{N-H}}$), 3046.2 (m, $\nu_{\text{C-H}}$), 1604.5 (s), 1565.6 (s), 1486.6 (vs, $\nu_{\text{C=C}}$), 738.5 (vs), 696.3 (s, $\delta_{\text{C-H}}$). Conductance ($\Omega^{-1}\text{cm}^2\text{mol}^{-1}$): 9.8.

p-HPIP: Yield: 88%. Anal. Found: C, 72.98; H, 3.94; N, 18.07; Calcd for C₁₉H₁₂N₄O: C, 73.07; H, 3.87; N, 17.94. ^1H NMR (DMSO- d_6 , 500 MHz) δ : 13.08 (s, 1H, -NH), 10.09 (s, 1H, -OH), 8.96 (d, 2H, $J = 7.9$ Hz, ArH), 8.84 (m, 2H, $J = 8.0$ Hz, ArH), 8.43 (d, 1H, $J = 8.2$ Hz, ArH), 7.77 (m, 2H, $J = 7.6$ Hz, ArH), 7.33 (s, 1H, ArH), 6.93 (d, 2H, $J = 8.0$ Hz, ArH). ^{13}C NMR (DMSO- d_6 , 500 MHz) δ : 158.5 C(2'), 151.4 C(13), 147.5 C(1, 10), 131.5 C(5, 6), 130.9 C(4, 7), 130.0 C(3, 8), 123.4 C(4', 6'), 121.8 C(4, 12), 120.9 C(5'), 119.5 C(2, 9), 116.9 C(1'), 113.5 C(3'). ES-MS: (CH₃OH): m/z 313.0 ([M + H]⁺). IR (KBr disk): ν (cm⁻¹) = 3498.9 (s, $\nu_{\text{O-H}}$), 3248.9 (s), 3217.7 (s, -NH₂), 3189.5 (s, $\nu_{\text{N-H}}$), 3034.9 (m, $\nu_{\text{C-H}}$), 1618.2 (s), 1578.4 (s), 1448.4 (vs, $\nu_{\text{C=C}}$), 742.2 (vs), 700.9 (s, $\delta_{\text{C-H}}$). Conductance ($\Omega^{-1}\text{cm}^2\text{mol}^{-1}$): 11.4.

Synthesis of [VO(hntdtsc)(HPIP)] (1)

This complex was synthesized by a mixture of HPIP (0.312 g, 1 mmol) and hntdtsc (0.245 g, 1 mmol) in absolute CH₃OH (60 mL) was heated at 80 °C under argon for 2h. After dissolution, an aqueous solution (10 mL) of 1.0 mmol (0.265 g) quantity of VO(acac)₂ was added dropwise to this mixture, and a green precipitate was formed. The solid power was purified by recrystallization in methanol, and dried *in vacuo*. Yield: 76%. Anal. Found: C, 60.08; H, 3.42; N, 15.69; Calcd for C₃₁H₂₁N₇O₃SV: C, 59.81; H, 3.40; N, 15.75. ^1H -NMR (DMSO- d_6 , 500MHz) δ : 12.65 (s, 1H, -NH), 11.40 (s, 1H, CH=N), 10.49 (s, 1H, -OH), 9.05 (d, 2H, $J = 8.5$ Hz, ArH), 8.42 (d, 2H, $J = 8.4$ Hz, ArH), 8.18 and 7.84 (2br s, 1H each NH₂), 8.12 (d, 2H, $J = 8.1$ Hz, ArH), 7.64 (d, 2H, ArH), 7.34-7.55 (m, 4H, $J = 7.8$ Hz, ArH), 7.11-7.24 (m, 4H, $J = 8.5$ Hz, ArH). ES-MS (CH₃OH): m/z : 623.0 ([M+H]⁺), 645.0 ([M + Na]⁺). IR (KBr disk): ν (cm⁻¹) = 3447.2 ($\nu_{\text{O-H}}$), 3338.4(s), 3275.1 (s, -NH₂), 3031.9 (m), 1573.2 (s), 1493.8 (s, $\nu_{\text{C=C-H}}$), 1612.9 (vs, $\nu_{\text{HC=N}}$), 1193.7 (m, $\nu_{\text{C-O}}$), 1086.1 (m, $\nu_{\text{C-N}}$), 952.0 (s, $\nu_{\text{V=O}}$), 821.8 (s), 755.9 (m, $\nu_{\text{C-S}}$), 731.9 (m, $\nu_{\text{V-N}}$). Conductance ($\Omega^{-1}\text{cm}^2\text{mol}^{-1}$): 13.6.

Synthesis of [VO(hntdtsc)(m-HPIP)] (2)

This complex was obtained by a similar procedure as for the complex 1, with *m*-HPIP (0.312 g, 1 mmol) in place of HPIP. Yield: 72%. Anal. Found: C, 60.02; H, 3.39; N, 15.79; Calcd for C₃₁H₂₁N₇O₃SV: C, 59.81; H, 3.40; N, 15.75. ^1H -NMR (DMSO- d_6 , 500MHz) δ : 14.31 (s, 1H, -NH), 10.18 (s, 1H, CH=N), 9.41 (s, 1H, -OH), 9.21 (d, 2H, $J = 8.5$ Hz, ArH), 8.13 (m, 4H, $J = 8.4$ Hz, ArH), 8.11 and 7.84 (2br s, 1H each NH₂), 7.50 (m, 4H, $J = 8.1$ Hz, ArH), 7.33 (d, 2H, $J = 8.1$ Hz, ArH), 7.00 (t, 4H, $J = 7.9$ Hz, ArH). ES-MS (CH₃OH): m/z : 623.0 ([M+H]⁺), 645.0

([M + Na]⁺). IR (KBr disk): ν (cm⁻¹) = 3444.7 ($\nu_{\text{O-H}}$), 3341.1 (s), 3200.2 (s, -NH₂), 3021.9 (m), 1597.1 (s), 1538.1 (s), 1491.4 (s, $\nu_{\text{C=C-H}}$), 1614.3 (vs, $\nu_{\text{HC=N}}$), 1195.3 (m, $\nu_{\text{C-O}}$), 1083.3 (m, $\nu_{\text{C-N}}$), 955.5 (s, $\nu_{\text{V=O}}$), 825.7 (s), 813.2 (m, $\nu_{\text{C-S}}$), 737.6 (m, $\nu_{\text{V-N}}$). Conductance ($\Omega^{-1}\text{cm}^2\text{mol}^{-1}$): 12.8.

Synthesis of [VO(hntdtsc)(p-HPIP)] (3)

This compound was synthesized by a similar procedure as for the complex 1, with *p*-HPIP (0.312 g, 1 mmol) in place of HPIP. Yield: 69%. Anal. Found: C, 59.68; H, 3.32; N, 15.77; Calcd for C₃₁H₂₁N₇O₃SV: C, 59.81; H, 3.40; N, 15.75. ^1H -NMR (DMSO- d_6 , 500MHz) δ : 13.73 (s, 1H, -NH), 12.40 (s, 1H, CH=N), 9.85 (s, 1H, -OH), 9.00 (d, 2H, $J = 8.6$ Hz, ArH), 8.84 (d, 2H, $J = 7.9$ Hz, ArH), 8.02 and 7.79 (2br s, 1H each NH₂), 7.57 (m, 4H, $J = 8.2$ Hz, ArH), 7.29 (t, 4H, $J = 8.2$ Hz, ArH), 7.08-6.86 (m, 4H, $J = 8.3$ Hz, ArH). ES-MS (CH₃OH): m/z : 623.0 ([M+H]⁺), 645.0 ([M + Na]⁺). IR (KBr disk): ν (cm⁻¹) = 3441.2 ($\nu_{\text{O-H}}$), 3333.0 (s), 3181.8 (s, -NH₂), 3034.8 (m), 1576.7 (s), 1538.8 (s), 1507.6 (s, $\nu_{\text{C=C-H}}$), 1616.1 (vs, $\nu_{\text{HC=N}}$), 1168.3 (m, $\nu_{\text{C-O}}$), 1079.0 (m, $\nu_{\text{C-N}}$), 965.1 (s, $\nu_{\text{V=O}}$), 825.7 (s), 812.1 (m, $\nu_{\text{C-S}}$), 731.0 (m, $\nu_{\text{V-N}}$). Conductance ($\Omega^{-1}\text{cm}^2\text{mol}^{-1}$): 18.1.

DNA-binding and photocleavage

The absorption titration of oxovanadium complexes in buffer A were performed at room temperature with a fixed concentration of the oxovanadium complex (20 mM) to which increments of DNA stock solutions were added. The oxovanadium-DNA solutions were incubated at room temperature for 5 min before the absorption spectra were recorded. In order to further elucidate the binding strength of the complex, the intrinsic binding constant K_b with CT-DNA was obtained by monitoring the change in the absorbance of the ligand transfer band with increasing amounts of DNA. K_b was then calculated using the following equation [13,20,28]

$$\frac{[DNA]}{\epsilon_a - \epsilon_f} = \frac{[DNA]}{\epsilon_b - \epsilon_f} + \frac{1}{K_b(\epsilon_b - \epsilon_f)}$$

Where [DNA] is the concentration of DNA in the base pairs, and ϵ_a , ϵ_f and ϵ_b refer to the corresponding apparent absorption coefficient $A_{\text{obsd}}/[\text{Vanadium}]$, the extinction coefficient for the free oxovanadium complex and the extinction coefficient for the oxovanadium complex in the fully bound form, respectively. In plots of [DNA]/($\epsilon_a - \epsilon_f$) versus [DNA], K_b is obtained by the ratio of the slope to the intercept.

Viscosity measurements were carried out with an Ubbelohde viscometer maintained at a constant temperature of (28.0 ± 0.1) °C in a thermostatic bath. Flow time was measured with a digital stopwatch, and each sample was measured five times to obtain the average flow time. Data are presented as (η/η_0)^{1/3} versus binding ratio [30], where η is the viscosity of DNA in the presence of complex while η_0 is the viscosity of DNA alone.

Thermal denaturation studies were carried out with Shimadzu UV-3101 PC spectrophotometer equipped with a Peltier temperature-controlling programmer (± 0.1°C). The melting temperature (T_m) was taken as the mid-point of the hyperchromic transition. The melting curves were obtained by measuring the absorbance at 260 nm for solutions of CT-DNA (80 μM) in the absence and presence of oxovanadium complex [20 μM] as a function of the temperature was scanned from 50 to 90 °C at a speed of 5°C min⁻¹. The data are presented as (A-A₀)/(A_f-A₀) versus T, where A, A₀ and A_f are the observed, the initial, and the final absorbance at 260 nm, respectively.

The cleavage activity of supercoiled pBR322 DNA by the oxovanadium complexes was studied by using agarose gel electrophoresis experiment, pBR322 DNA (0.1 μg) was treated with the

complex in buffer B in different concentrations, and the solutions were incubated at 37°C in the incubator for 1h. The samples were analyzed by electrophoresis for 2h at 90 V in tris-boric buffer containing 0.8% agarose gel. The gel was stained with 0.1 µg/mL DuRed nucleic acid gel stain and photographed under UV light on an Alpha Innotech IS-5500 fluorescence chemiluminescence and visible imaging system [19,20,31].

Cell viability assay

3-(4,5-Dimethylthiazole)-2,5-diphenyltetrazolium bromide (MTT) dye assay was carried out to evaluate cytotoxicity in human CaSki, SiHa, K562, HepG2, EC9706 and EC109 cell lines. Cells were seeded in 96-well microassay culture plates (2×10^4 cells per well) and incubated at 37 °C in a 5% CO₂ atmosphere for 48h. The compounds tested were then added to the wells to achieve final concentration ranging 10^{-6} to 10^{-4} mol L⁻¹. Control wells were prepared by addition of culture medium (100 µL). Wells containing culture medium without cells were used as blanks. Upon completion of the incubation, then stock MTT dye solution (20 µL, 5 mg mL⁻¹) was added to each well. After 4 h incubation, a solution containing N, N-dimethylformamide (50%) and sodium dodecyl sulfate (20%) was added to solubilize the MTT formazan. The cell viability of each well was then measured on a Multiskan SSCENT microplate reader at 490 nm. The IC₅₀ values were determined by plotting the percentage viability versus concentration on a logarithmic graph and reading off the concentration at which 50% of cells remain viable relative to the control [32]. Each experiment was repeated at least three times to get the mean values.

Results and Discussion

Synthesis of ligands and V-complexes

The phenanthroline-based derivatives ligands were prepared by the reaction of 1,10-phenanthroline-5,6-dione with hydroxybenzaldehyde in the appropriate mole ratios in the presence of ammonium acetate using glacial acetic acid as solvent. The oxovanadium complexes 1-3 were synthesized by refluxing of corresponding ligand, VO(acac)₂ and phenanthroline-based ligand in absolute methanol. The desired complexes were purified by recrystallization.

In the IR spectra of phenanthroline-based ligands show absorption at ca. 3340 cm⁻¹ (ν_{O-H}), 3200 cm⁻¹ (imidazole N-H), 3040 cm⁻¹ (ν_{C=C-H}), 1448-1618 cm⁻¹ (ν_{C=C}), 740 cm⁻¹, 700 cm⁻¹ (δ_{C-H}), respectively. In parallel, IR spectra absorption of complexes 1-3 observed at ca. 3440 cm⁻¹ (ν_{O-H}), 3180 cm⁻¹ and 3340 cm⁻¹ is assigned to (-NH₂), 3030 cm⁻¹ (ν_{C=C-H}), 1490-1580 cm⁻¹ (ν_{C=C}), 1612-1616 cm⁻¹ (ν_{CH=N}), 1312 cm⁻¹, 810-313 (ν_{C-S}), 731-737 cm⁻¹ for (ν_{V-N}), which indicates both two mixed ligands are coordinated to vanadium. The strong (ν_{V=O}) band at 956-974 cm⁻¹ observed at oxovanadium complexes, which is not present in the spectrum of free ligands could be clearly identified for the formulation of the complex [33-34].

Electronic spectra of complexes 1-3 show an intense band at ca. 268 nm assignable to π→π* transition of aromatic rings of phenanthroline-based ligands [35-36]. The remaining bands in the UV-vis region (320-330 nm) are attributed to intraligand transitions of the Schiff base. The obtained spectral data indicates the Schiff base bonded through the phenolate oxygen, imine nitrogen and thiolate sulfur atoms leaving the thiomethyl as the pendant group. These values are close to the reported values for a square-pyramidal geometry [19,28,37] and it also suggested that these complexes bear the central V (IV) atom with coordination numbers 5 in a square-pyramidal geometry.

In the ¹H NMR spectra of phenanthroline-based ligands showed peaks of aromatic hydrogen (ArH), imidazole secondary amine (NH)

proton. However, in the ¹H NMR spectra of complexes, the peaks of imine (CH=N) proton and primary amine (-NH₂) were observed, which affirmed that the Schiff base ligand was coordinated to vanadium.

According to the ES-MS spectra, the molecular ion peaks of three complexes appearing at m/z 623.0 ([M+H]⁺) and 645.0 ([M+Na]⁺). Elemental analysis, ES-MS, IR and ¹H NMR data of all the compounds are in good agreement with the expected structures.

The molar conductance values of phenanthroline-based ligands and complexes 1-3 in DMF (1 mM) are shown in Table 1. The conductive properties indicate that both oxovanadium complexes and the corresponding ligands are nonelectrolytes.

Electronic absorption titration

Electronic absorption spectral titration is one of the most common ways to investigate the interactions of compounds with DNA. To further evaluate the capacity of oxovanadium complexes interacting with CT-DNA, the electronic absorption spectra of complexes 1-3 are characterized by intense π-π* transition of aromatic rings in the absence and presence of increasing concentration of CT-DNA, which are shown in Figure 1. Complexes bind to the pairs base of DNA by π-π* stacking interactions between the planar aromatic chromophore of the complexes and the base pairs of DNA usually result in hypochromism and bathochromism [13,20,28]. As can be seen in Figure 1, with the CT-DNA concentration increasing, obvious hypochromism as well as a certain degree of bathochromism for the oxovanadium complex 1-3 can be observed in the ultraviolet titration process. The appreciable hypochromism and bathochromism for complex 1 is 56.17% and 3 nm at 272 nm. In contrast, a slighter hypochromism can be observed for complexes 2 and 3, which exhibit 12.53% and 25.23%, respectively, and also bathochromism of 1 nm at 268 nm and 1.5 nm at 270 nm, respectively. According to previously reported results [13,19,24], the UV-Vis spectral characteristics suggest that complexes 1-3 interact with CT-DNA most likely through a mode that involves a stacking interaction between the aromatic chromophore and the base pairs of DNA.

In order to compare quantitatively the DNA-binding strengths of these complexes, the intrinsic binding constant K_b was calculated from the changes in absorbance in the ligand charge transfer bands with increasing amounts of CT-DNA. The value of K_b were calculated as well using the equation, reaching $(4.38 \pm 0.01) \times 10^5 \text{ M}^{-1}$, $(1.07 \pm 0.01) \times 10^5 \text{ M}^{-1}$ and $(1.83 \pm 0.01) \times 10^5 \text{ M}^{-1}$ for complexes 1, 2 and 3, respectively. The K_b values indicate that oxovanadium complexes 1-3 interact with CT-DNA by intercalation modes. It is interesting to note that the DNA-binding affinities of complexes 1, 2 and 3 are stronger than that of the reported oxovanadium complexes, such as VO(SAA)(phen) ($4.50 \times 10^4 \text{ M}^{-1}$), VO(MOSAA)(phen) ($2.95 \times 10^4 \text{ M}^{-1}$) [19] and VO(hntdtsc)(phen) ($8.2 \times 10^4 \text{ M}^{-1}$) [28], under our experimental conditions. This may due to the introduction of imidazole ring in auxiliary ligands substituted with 1, 10-phenanthroline, which leads to formation of a richer conjugated aromatic structure, thus resulting in stronger insertion into DNA. Meanwhile, the presence of an -OH group on the aromatic moieties, which acts as an electron-donating

Compounds	Ω ⁻¹ cm ² mol ⁻¹
HPIP	8.6
m-HHPIP	9.8
p-HPIP	11.4
VO(hntdtsc)(HPIP)	13.6
VO(hntdtsc)(m-HPIP)	12.8
VO(hntdtsc)(p-HPIP)	18.1

Table 1: Molar conductivity data of oxovanadium complexes and ligands.

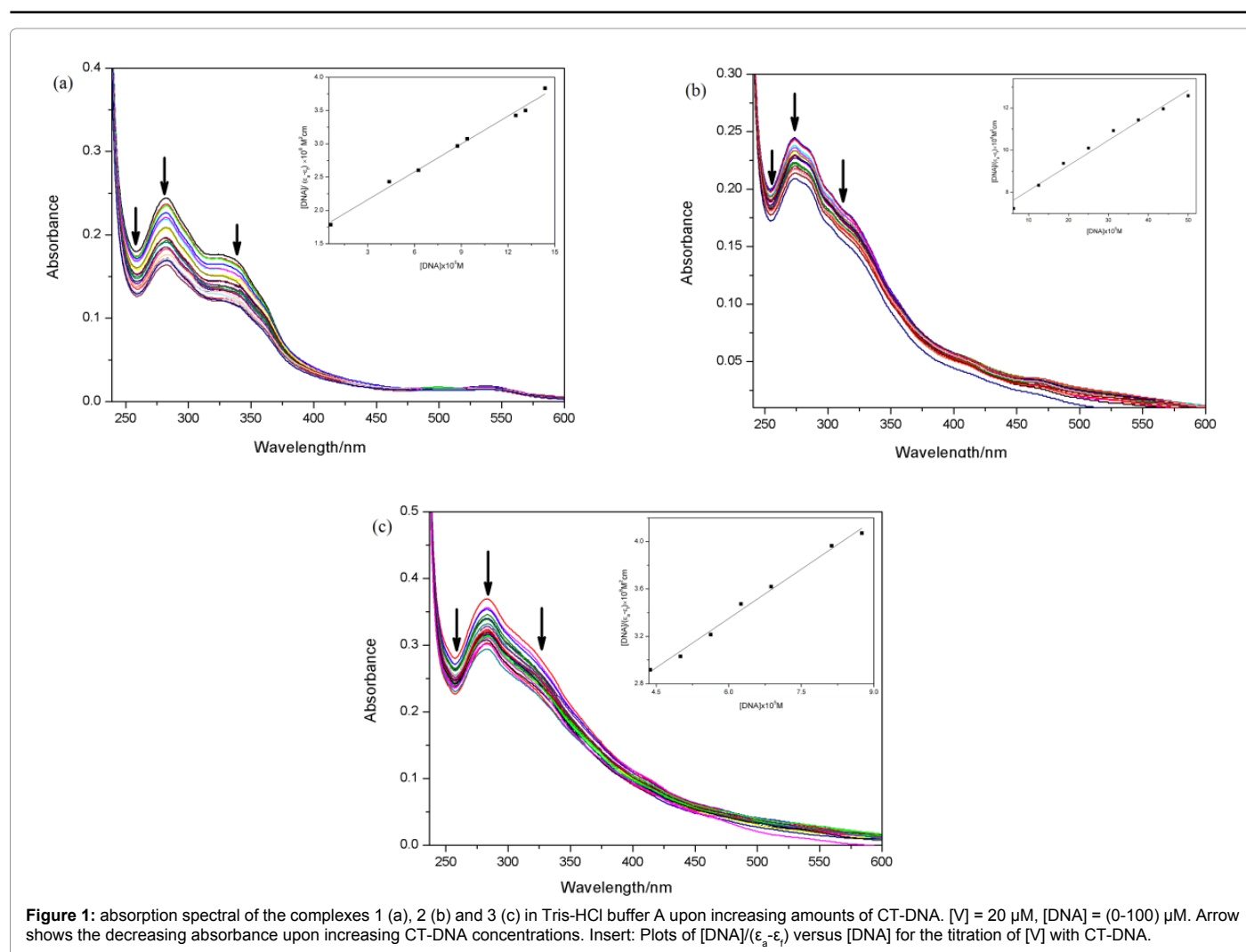


Figure 1: absorption spectral of the complexes 1 (a), 2 (b) and 3 (c) in Tris-HCl buffer A upon increasing amounts of CT-DNA. $[V] = 20 \mu\text{M}$, $[\text{DNA}] = (0-100) \mu\text{M}$. Arrow shows the decreasing absorbance upon increasing CT-DNA concentrations. Insert: Plots of $[\text{DNA}]/(\epsilon_a - \epsilon_f)$ versus $[\text{DNA}]$ for the titration of $[V]$ with CT-DNA.

substituent on the intercalative ligand and thus gives stronger stacking interactions with DNA.

The intrinsic binding constant, K_b increase in the order $2 < 3 < 1$. Interestingly, from a comparison of the DNA-binding activities of complexes 1, 2 and 3, the complex 1 appeared to be a much stronger DNA intercalator. The differences of their binding strength may due to the changes in the electronic characteristics of substituted group at the different locations introduced on the aromatic ring of phenanthroline-based ligands, which may make differences in the DNA-binding affinities. The results also indicates an -OH group substituted on the ortho-position of the aromatic ring exhibits stronger DNA-binding affinity than substituted on the *para*-position and meta-position [19,28]. And it thus provides strong evidence for the electronic effect of phenanthroline is one of the factors in determining the binding affinities.

Fluorescence spectroscopic studies

The interaction of the complexes ($20 \mu\text{mol L}^{-1}$) with CT-DNA was investigated using fluorescence emission titration experiment in the Tris buffer A at room temperature. The emission spectra of complexes 1, 2 and 3 in the absence and presence of CT-DNA exhibit luminescence in Tris buffer A, with a maxima appearing at 296 nm, 656 nm and 697 nm respectively, which are shown in Figure 2. Emission intensity of complexes 1-3 is found to depend on DNA concentration.

Upon increasing concentrations of CT-DNA, the emission intensities of complexes 1-3 grow to around by about 1.21, 0.38, and 0.64 times larger than those in the absence of CT-DNA and saturates at a $[\text{DNA}]/[V]$ ratio of 20 : 1. The enhancement of emission intensity is an indication of binding of the complexes to the hydrophobic pocket of DNA, since the hydrophobic environment inside the DNA helix reduces the accessibility of water molecules to the complex and the complex mobility is restricted at the binding site, leading to decrease of the vibrational modes of relaxation [38]. The fluorescence spectroscopic data shows that 1 interacts with CT-DNA more strongly than both 1 and 2, consistent with the UV-Vis absorption titration spectral results.

Viscosity measurements

Viscosity measurements are regarded as the least controversial and the most rigorous means of testing the binding mode of DNA in solution [19,28]. To further clarify the DNA-binding mode of complexes 1-3, viscosity measurements on solutions of CT-DNA incubated with the complexes were performed. It is well-known that a classical intercalation model leads to an apparent increase in viscosity of DNA solution due to base-pairs are pushed apart and hence an increase in overall DNA length. In contrast, a partial, non-classical intercalation of compounds could bend (or kink) the DNA helix and reduce its effective length and, concomitantly, its viscosity [19,20,24].

The effects of complexes 1-3 on the viscosity of CT-DNA are shown

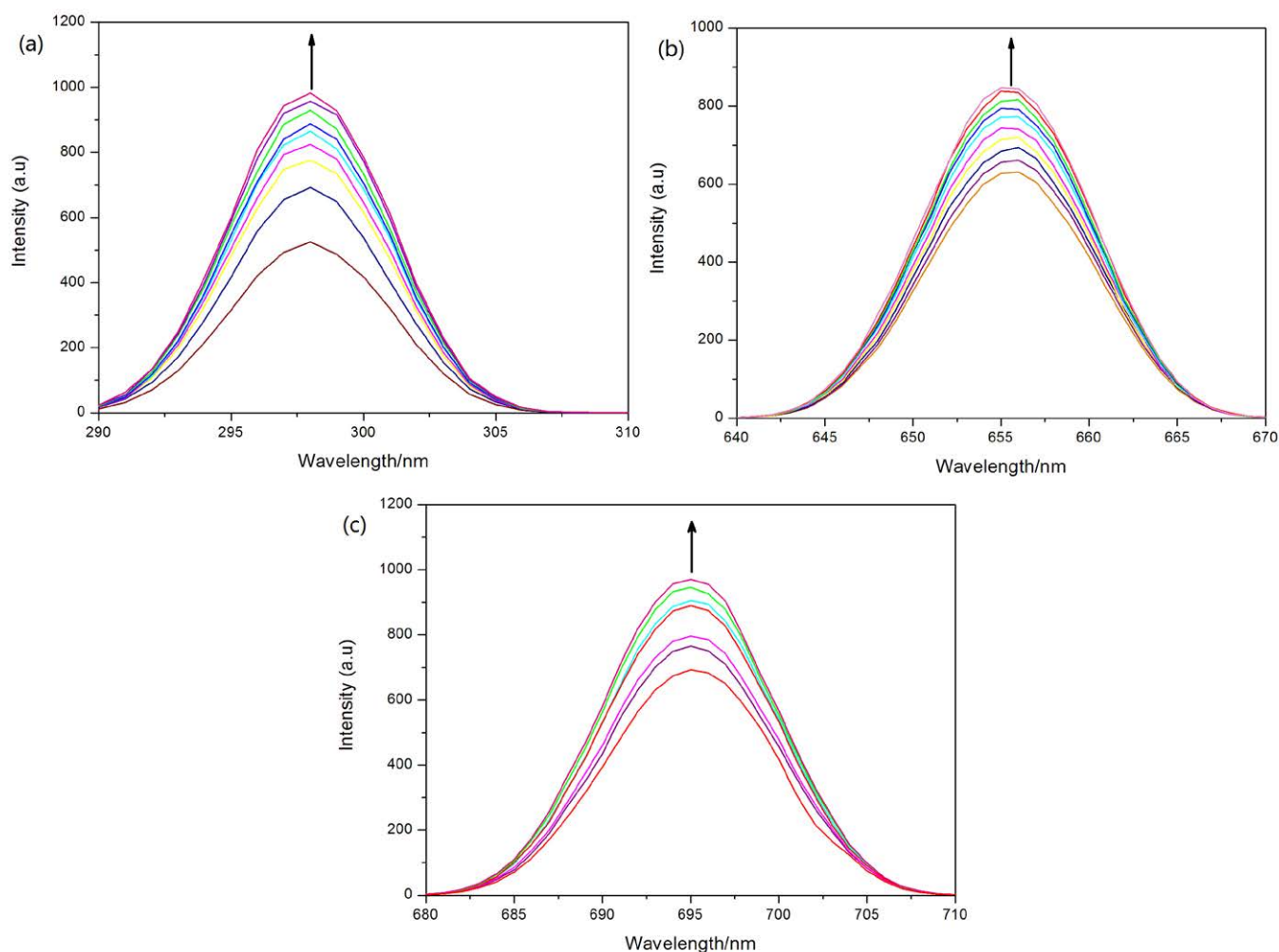


Figure 2: Emission spectra of 1 (a), 2 (b) and 3 (c) in Tris-HCl buffer A in the absence and presence of CT-DNA. $[V] = 20 \mu\text{mol L}^{-1}$. Arrows show the increasing intensity with increasing concentrations of DNA.

in Figure 3. As can be seen in Figure 3, with amounts of the complexes increasing, the relative viscosity of DNA increases continuously to some extent. The results thus provide strong evidence for the interaction of complexes 1-3 with CT-DNA by intercalation modes. Moreover, the large increase in the relative viscosity revealed that 1 is a better intercalator than 2 and 3, which is consistent with our foregoing hypothesis that electronic effects of introduction of larger planar aromatic rings on phenanthroline-based ligands play a key role in DNA-binding affinities.

Thermal denaturation studies

DNA melting experiments are generally applied to investigate the extent of intercalation, which were carried out by monitoring the intensity of DNA bases at 260 nm at different temperatures, both in the absence and presence of oxovanadium complex and ligands. Thermal behaviors of DNA in the presence of compounds can give insight into their conformational changes when the temperature is raised and offer information about the interaction strength of complexes with DNA. With the temperature in the solution rising, the double-stranded DNA will gradually dissociate to single strands and generate a hyperchromic effect on absorption spectra of DNA bases. Thus, the melting temperature T_m , which is defined as the temperature where half of the total base pairs are unbound, is usually introduced. Generally,

T_m will increase considerable when intercalative binding occurs, since intercalation of the complex into DNA base pairs causes stabilization of base stacking and hence raises the melting temperature of the double-stranded DNA [13,24,28].

The melting curves of CT-DNA in the absence and presence of complexes 1, 2 and 3 are shown in Figure 4. As can be seen from Figure 4, the T_m of CT-DNA in the absence of the complex is $61.6 \pm 0.2^\circ\text{C}$, meanwhile, when the complexes at a concentration ratio $[V]/[\text{DNA}]$ of 1:4, we can observe that T_m values in the presence of the complexes 1-3 are $71.4 \pm 0.2^\circ\text{C}$, $64.7 \pm 0.2^\circ\text{C}$ and $67.8 \pm 0.2^\circ\text{C}$, respectively. A comparison of the ΔT_m values of the complex and its ligands (9.8°C , 3.1°C and 6.2°C , respectively) was agreement with those classical intercalators [19,20,24,28], which provided strong evidence for their binding with DNA by intercalation modes.

The experimental data reveals that oxovanadium complexes in collaboration with Schiff base and imidazole[4,5-f][1,10]phenanthroline-based ligands exhibit appreciable DNA intercalative activities, it is quite consistent with their binding abilities with CT-DNA.

Photocleavage studies

The interaction mode between the oxovanadium complex and

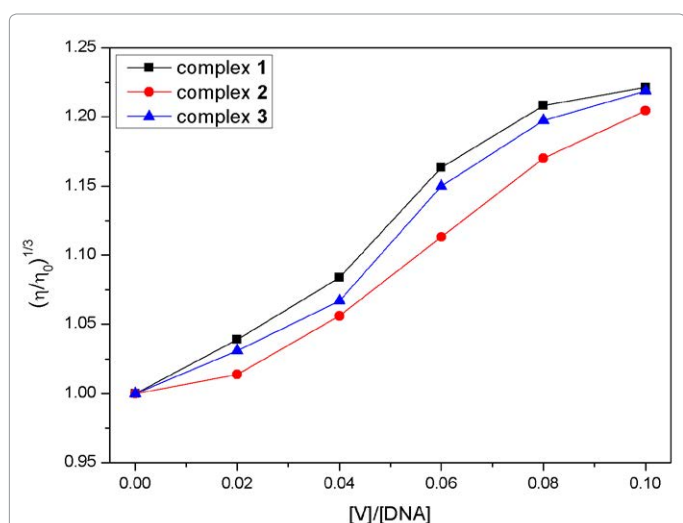


Figure 3: Effect of increasing amounts of complexes 1 (■), 2 (●) and 3 (▲) on the relative viscosity of CT-DNA at (28.0 ± 0.1) °C, [DNA] = 0.2 mmol L⁻¹.

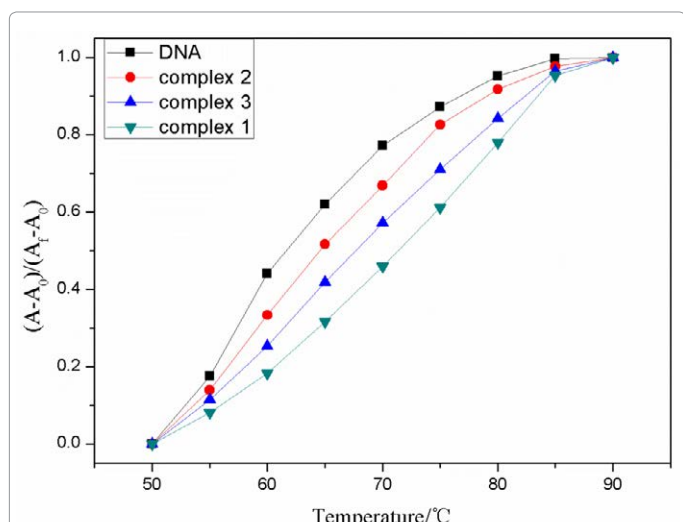


Figure 4: Thermal denaturation of CT-DNA in the absence and presence of complexes 1 (▼), 2 (●) and 3 (▲), [V] = 20 μM, [DNA] = 80 μM.

plasmid DNA was further investigated by agarose gel electrophoresis experiments. When circular plasmid DNA is subject to electrophoresis, relatively fast migration will be observed for the intact supercoiled form (form I). If scission occurs on one strand (nicking), the supercoil will relax to generate a slower moving open circular form (form II). If both strands are cleaved, a linear form (form III) will be generated [39]. The cleavage reactions on plasmid DNA induced by oxovanadium complexes were investigated and monitored by gel electrophoresis experiments.

As is shown both in Figure 5 and 6, it is clear to figure out the cleavage activity of plasmid pBR322 DNA after incubation with different concentrations of V-complexes at 37°C for 1 h at dark condition. The nicked form II can barely be observed for H₂O₂ alone in the absence of the complexes (lane 2 in Figures 5 and 6, respectively). Nevertheless, in the presence of complexes 1, 2 and 3 with 30 mM H₂O₂, apparent cleavage of pBR322 DNA observed from the formation of form II, and cleaving activity tends to increase gradually with the concentration of the complexes increase from 15 μmol L⁻¹ to 60 μM (lane 3, 4 and 5 in Figures 5 and 6). Furthermore, under the same conditions with lane 4,

addition of 0.02 mol L⁻¹ L-Histidine works as a singlet oxygen quencher (lane 6, lane 11 in Figures 5 and 6, respectively) slightly inhibits the cleavage of DNA. Meanwhile, no cleavage of plasmid DNA occurred in the presence of hydroxyl radical scavenger DMSO (lane 7, lane 12 in Figures 5 and 6, respectively), suggesting that ·OH radicals is likely to be the reactive species on account of the oxidation of VO²⁺ in the presence of H₂O₂ for the cleavage reaction [19,24,28]. Under comparative experimental conditions, the cleavage ability follows the order of 1 > 3 > 2. The results are actually consistent with the degree of their intrinsic binding constant (*K_b*), indicating that the introduction of imidazole ring on the auxiliary ligands substituted with 1,10-phenanthroline as well as electrochemical characteristics of the existence of substituted electronic-donating group (-OH) at the different locations introduced on the aromatic ring of phenanthroline-based ligands makes a big difference in the DNA-binding affinity.

In vitro cytotoxicity assays

The cytotoxicity *in vitro* assay for complexes 1-3 against cervical cancer CaSki and SiHa, leukemia K562, HepG2, esophagus carcinoma EC9706 and EC109 cell lines were evaluated by MTT assay. The inhibitory percentage against growth of cancer cells was determined. The cell viabilities (%) obtained with continuous exposure for 48 h are depicted in Figure 7. Cell viability decreased with increasing concentrations of 1-3. The IC₅₀ values were calculated and are listed in Table 2. As shown in Table 2, three oxovanadium complexes exhibit broad inhibition of tested cancer cell lines, with IC₅₀ values ranging from 0.41 to 89.2 μM, and the cytotoxicity was concentration-dependent.

It is notable that complex 1 possessed the most potent cytotoxicity against the cell lines of CaSki, SiHa, K562, HepG2, EC9706 and EC109. Although complexes 2 and 3 appeared to be less antiproliferative activity towards HepG2, complex 1 still show high inhibitory effect, which IC₅₀ values reaches to 0.73 μM. This is consistent with its binding abilities with CT-DNA, indicating that the antitumor abilities of the oxovanadium complexes may be closely related to their DNA binding mode.

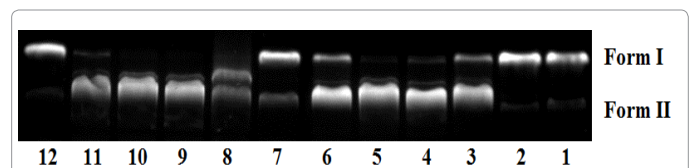


Figure 5: Cleavage of pBR322 DNA by complexes 2 and 3 (15-60 μM) in the absence and presence of H₂O₂ (30 mM) in buffer B (pH 7.2). lane 1, DNA control; lane 2, DNA + H₂O₂; lane 3, DNA + 2 (15 μM) + H₂O₂; lane 4, DNA + 2 (30 μM) + H₂O₂; lane 5, DNA + 2 (60 μM) + H₂O₂; lane 6, DNA + 2 (30 μM) + H₂O₂ + L-Histidine (0.02 M); lane 7, DNA + 2 (30 μM) + H₂O₂ + DMSO (2 μL); lane 8, DNA + 3 (15 μM) + H₂O₂; lane 9, DNA + 3 (30 μM) + H₂O₂; lane 10, DNA + 3 (60 μM) + H₂O₂; lane 11, DNA + 3 (30 μM) + H₂O₂ + L-Histidine (0.02 M); lane 12, DNA + 3 (30 μM) + H₂O₂ + DMSO (2 μL).

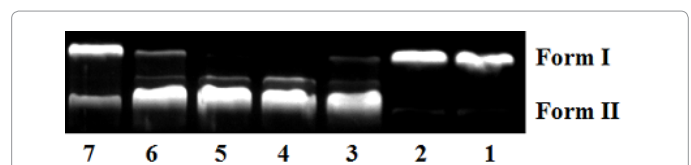
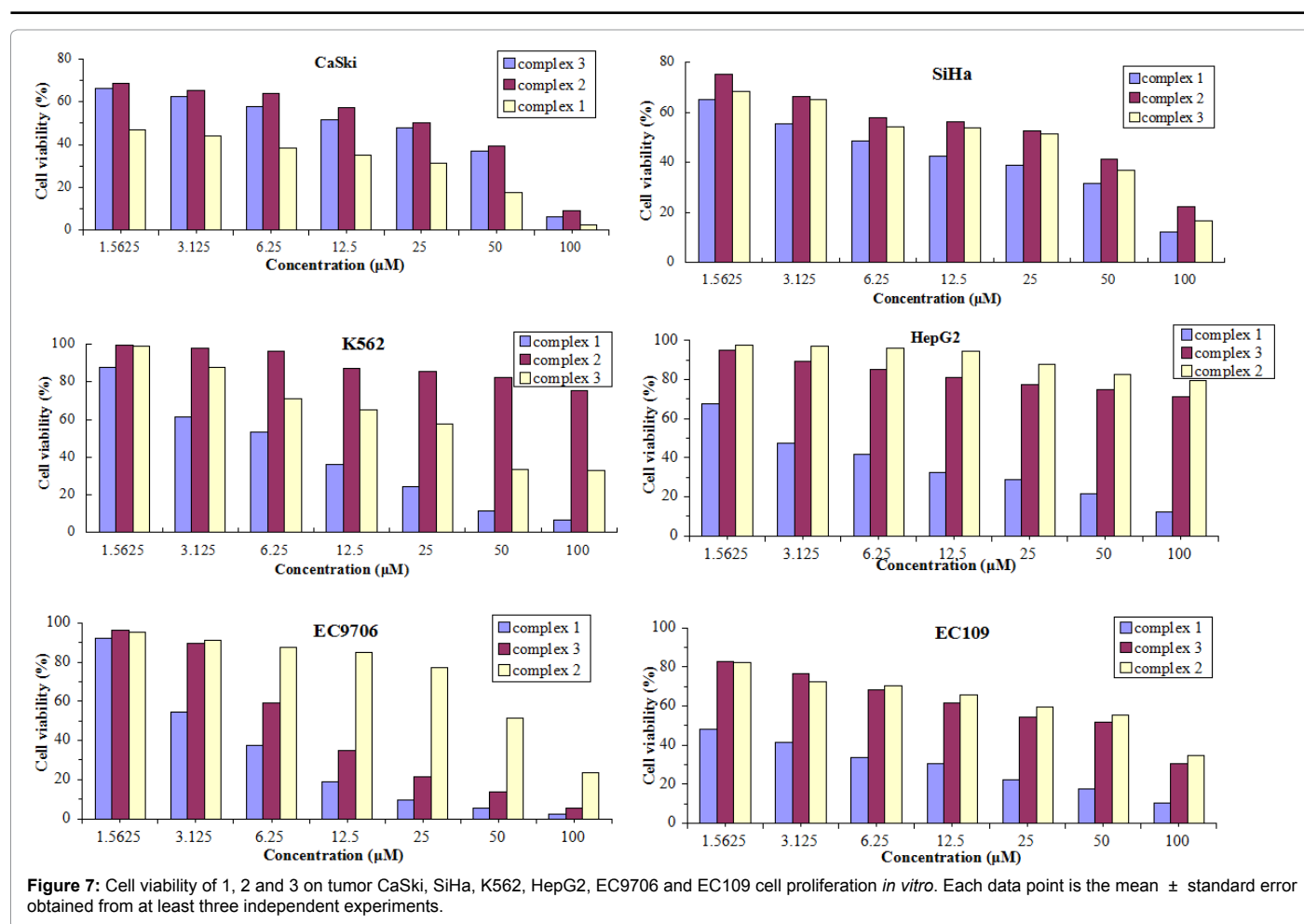


Figure 6: Cleavage of pBR322 DNA by complex 1 (15-60 μM) in the absence and presence of H₂O₂ (30 mM) in buffer B (pH 7.2). lane 1, DNA control; lane 2, DNA + H₂O₂; lane 3, DNA + 1 (15 μM) + H₂O₂; lane 4, DNA + 1 (30 μM) + H₂O₂; lane 5, DNA + 1 (60 μM) + H₂O₂; lane 6, DNA + 1 (30 μM) + H₂O₂ + L-Histidine (0.02 M); lane 7, DNA + 1 (30 μM) + H₂O₂ + DMSO (2 μL).



Compounds	IC ₅₀ (μM)					
	CaSki	SiHa	K562	Hep G2	EC9706	EC109
Complex 1	0.69 \pm 0.1	5.5 \pm 0.4	3.6 \pm 0.2	0.73 \pm 0.2	4.7 \pm 0.8	0.41 \pm 0.1
Complex 2	11.2 \pm 1.1	10.2 \pm 1.3	51.9 \pm 2.6	>100	11.6 \pm 1.1	22.8 \pm 1.8
Complex 3	22.8 \pm 1.4	20.7 \pm 1.7	>100	>100	14.2 \pm 2.3	89.2 \pm 3.4

Table 2: The IC₅₀ values for 1, 2 and 3 against selected cell lines.

Conclusion

In this paper, three oxovanadium complexes incorporating Schiff base and phenanthroline-based ligands have been synthesized and characterized. Their DNA-binding activities with CT-DNA indicate that they bind to DNA by intercalation modes and the DNA-binding affinity follows the order 1>3>2. These oxovanadium complexes can cause DNA cleavage. The results imply that the interaction with DNA may be closed associated with the introduction of imidazole ring in auxiliary ligands substituted with 1,10-phenanthroline as well as the electronic effects of substituted electronic-donating group (-OH) at the different locations introduced on the aromatic ring of phenanthroline-based ligands makes a big difference in the DNA-binding affinity. Furthermore, they also show highly cytotoxic activities against cervical, leukemia, Hepatoma and esophagus carcinoma cell lines. Complex 1 was found to be the most potent antitumor agent among the three complexes. Further investigation is required to study the possible cytotoxicity mechanisms of these complexes.

Acknowledgements

We gratefully acknowledge financial support for this work by the Science and

technology Research Project of Guangdong Province (No.2012B031800431), P. R. China and Cultivation of Natural Science Joint Fund of the First Affiliated Hospital and the Scientific & Technical Department of Guangdong Pharmaceutical University (No. 2014-36).

References

1. Srishaliam A, Kumar YP, Venkat Reddy P, Nambigari N, Vuruputuri U, et al. (2014) Cellular uptake, cytotoxicity, apoptosis, DNA-binding, photocleavage and molecular docking studies of ruthenium(II) polypyridyl complexes. *J Photochem Photobiol B* 132: 111-123.
2. Liu ML, Jiang M, Zheng K, Li YT, Wu ZY, et al. (2014) Synthesis and structure of a new mononuclear copper(II) complex with 2,2'-bipyridine and picrate: molecular docking, DNA-binding, and *in vitro* anticancer activity. *J Coord Chem* 67: 630-648.
3. Basu Baul TS, Kundu S, Linden A, Raviprakash N, Manna SK, et al. (2014) Synthesis and characterization of some water soluble Zn(II) complexes with (E)-N-(pyridin-2-ylmethylene)arylamines that regulate tumour cell death by interacting with DNA. *Dalton Trans* 43: 1191-1202.
4. Guin PS, Mandal PC, Das S (2012) A comparative study on the interaction with calf thymus DNA of a Ni(II) complex of the anticancer drug adriamycin and a Ni(II) complex of sodium 1,4-dihydroxy-9,10-anthraquinone-2-sulphonate. *J Coord Chem* 65: 705-721.
5. Wang QX, Gao F, Gao F, Li SX, Weng W, et al. (2012) A novel hybridization

- indicator for the low-background detection of short DNA fragments based on an electrically neutral cobalt(II) complex. *Biosens Bioelectron* 32: 50-55.
- Nielsen FH (1998) The nutritional essentiality and physiological metabolism of vanadium in higher animals. *ACS Symp Ser* 711: 297-307.
 - Morsy MD, Abdel-Razek HA, Osman OM (2011) Effect of vanadium on renal Na⁺,K⁺-ATPase activity in diabetic rats: a possible role of leptin. *J Physiol Biochem* 67: 61-69.
 - Zwolak I (2014) Vanadium carcinogenic, immunotoxic and neurotoxic effects: a review of *in vitro* studies. *Toxicol Mech Methods* 24: 1-12.
 - Anupama B, Gyana KC (2011) Synthesis, characterization, DNA binding and antimicrobial activity of 4-amino antipyrine Schiff base metal complexes. *Res J Pharm Biol Chem Sci* 2: 140-159.
 - Walmsley RS, Litwinski C, Antunes E, Hlangothi P, Hosten E, et al. (2013) Oxovanadium(IV)-containing poly(styrene-co-4'-ethenyl-2-hydroxyphenylimidazole) electrospun nanofibers for the catalytic oxidation of thioanisole. *J Mol Catal A: Chem* 379: 94-102.
 - Sanna D, Micera G, Garribba E (2013) Interaction of insulin-enhancing vanadium compounds with human serum holo-transferrin. *Inorg Chem* 52: 11975-11985.
 - Yamaguchi T, Watanabe S, Matsumura Y, Tokuoka Y, Yokoyama A (2012) Oxovanadium complexes with quinoline and pyridinone ligands: syntheses of the complexes and effect of alkyl chains on their apoptosis-inducing activity in leukemia cells. *Bioorg Med Chem* 20: 3058-3064.
 - Liao X, Pan W, He R, Guo H, Ying P, et al. (2014) Unsymmetrical oxovanadium complexes derived from salicylaldehyde and phenanthroline: synthesis, DNA interactions, and antitumor activities. *Chem Biol Drug Des* 83: 367-378.
 - Khatun R, Islam ASMA, Hai MA (2012) Synthesis of Schiff base having a heterocyclic moiety along with its cyclized derivatives and study of their antifungal activities. *J Bangladesh Chem Soc* 25: 7-14.
 - Ali AQ, Teoh SG, Salhin A, Eltayeb NE, Khadeer Ahamed MB, et al. (2014) Synthesis of isatin thiosemicarbazones derivatives: *in vitro* anti-cancer, DNA binding and cleavage activities. *Spectrochim Acta A Mol Biomol Spectrosc* 125: 440-448.
 - Rai BK, Kumari R (2013) Synthesis, structural, spectroscopic and antibacterial studies of Schiff base ligands and their metal complexes containing nitrogen and sulphur donor atom. *Orient J Chem* 29: 1163-1167.
 - Abbas SY, Farag AA, Ammar YA, Atrees AA, Mohamed AF, et al. (2013) Synthesis, characterization, and antiviral activity of novel fluorinated isatin derivatives. *Monatsh Chem* 144: 1725-1733.
 - Maia PIDS, Pavan FR, Leite CQF, Lemos SS, de Sousa GF, et al. (2009) Vanadium complexes with thiosemicarbazones: Synthesis, characterization, crystal structures and anti-*Mycobacterium tuberculosis* activity. *Polyhedron* 28: 398-406.
 - Guo HW, Lu JZ, Ruan ZG, Zhang YL, Liu YJ, et al. (2012) Synthesis, DNA-binding, cytotoxicity, and cleavage studies of unsymmetrical oxovanadium complexes. *J Coord Chem* 65: 191-204.
 - Lu JZ, Du YF, Guo HW, Jiang J, Zeng XD, et al. (2011) Two oxovanadium complexes incorporating thiosemicarbazones: synthesis, characterization, and DNA-binding studies. *J Coord Chem* 64: 1229-1239.
 - Jin, XP, Zhang L, Gao HQ, Fang JH, Li RF, et al. (2013) Palladium- and copper-catalyzed cross coupling reaction of aliphatic alcohols and aryl halides. *Huaxue Jinzhan* 25: 1898-1905.
 - Martinez Medina JJ, Islas MS, Lopez Tevez LL, Ferrer EG, Okulik NB, et al. (2014) Copper(II) complexes with cyanoguanidine and o-phenanthroline: Theoretical studies, *in vitro* antimicrobial activity and alkaline phosphatase inhibitory effect. *J Mol Struct* 1058: 298-307.
 - Anbu S, Killovalavan S, Alegria ECBA, Mathan G, Kandaswamy M (2013) Effect of 1,10-phenanthroline on DNA binding, DNA cleavage, cytotoxic and lactate dehydrogenase inhibition properties of Robson type macrocyclic dicopper(II) complex. *J Coord Chem* 66: 3989-4003.
 - Liu YJ, Li ZZ, Liang ZH, Yao JH, Huang HL (2011) Cytotoxicity, apoptosis, cellular uptake, cell cycle arrest, photocleavage, and antioxidant activity of 1,10-phenanthroline ruthenium(II) complexes. *DNA Cell Biol* 30: 839-848.
 - Kalia SB, Kaushal G, Kumar M, Cameotra SS, Sharma A, et al. (2009) Antimicrobial and toxicological studies of some metal complexes of 4-methylpiperazine-1-carbodithioate and phenanthroline mixed ligands. *Braz J Microbiol* 40: 916-922.
 - Bonello RO, Morgan IR, Yeo BR, Jones LEJ, Kariuki BM, et al. (2014) Luminescent rhenium(I) complexes of substituted imidazole[4,5-f]-1,10-phenanthroline derivatives. *Journal of Organometallic Chemistry* 749: 150-156.
 - Gomleksiz M, Alkan C, Erdem B (2013) Synthesis, characterization and antibacterial activity of imidazole derivatives of 1,10-phenanthroline and their Cu(II), Co(II) and Ni(II) complexes. *S Afr J Chem* 66: 107-112.
 - Lu J1, Guo H, Zeng X, Zhang Y, Zhao P, et al. (2012) Synthesis and characterization of unsymmetrical oxidovanadium complexes: DNA-binding, cleavage studies and antitumor activities. *J Inorg Biochem* 112: 39-48.
 - Cai ZB, Liu LF, Hong YQ, Zhou M (2013) Synthesis, characterization, and nonlinear optical responses of nickel(II) complexes with phenanthroline-based ligands. *J Coord Chem* 66: 2388-2397.
 - Tabatabaee M, Bordbar M, Ghassemzadeh M, Tahrii M, Tahrii M, et al. (2013) Two new neutral copper(II) complexes with dipicolinic acid and 3-amino-1H-12,4-triazole formed under different reaction conditions: Synthesis, characterization, molecular structures and DNA-binding studies. *Eur J Med Chem* 70: 364-371.
 - Hazari PP1, Pandey AK, Chaturvedi S, Tiwari AK, Chandna S, et al. (2013) Two new neutral copper(II) complexes with dipicolinic acid and 3-amino-C-substituted diamines and pyridoxal-5-phosphate as antitumor agents. *Chem Biol Drug Des* 79: 223-234.
 - Masango MG, Ferreira GC, Ellis CE, Elgorashi EE, Botha CJ (2014) Cytotoxicity of diplodiatoxin, dipmatol and diploine, metabolites synthesized by *Stenocarpella maydis*. *Toxicon* 82: 26-29.
 - Jabeen M, Ali S, Shahzadi S, Sharma SK, Qanungo K (2014) Synthesis, characterization, theoretical study and biological activities of oxovanadium (IV) complexes with 2-thiophene carboxylic acid hydrazide. *J Photochem Photobiol B* 136: 34-45.
 - Chen C, Bai FY, Zhang R, Song G, Shan H, et al. (2013) Synthesis, structure, and catalytic bromination of supramolecular oxovanadium complexes containing oxalate. *J Coord Chem* 66: 671-688.
 - Nejo AA, Kolawole GA, Opoku AR, Wolowska J, Brien PO (2009) Synthesis, characterization and preliminary insulin-enhancing studies of symmetrical tetradentate Schiff base complexes of oxovanadium(IV). *Inorganica Chimica Acta* 362: 3993-4001.
 - Yang PJ, Cui FJ, Yang XJ, Wu B (2013) Syntheses and Structures of Mononuclear, Dinuclear and Polynuclear Silver(I) Complexes of 2-Pyrazole-Substituted 1,10-Phenanthroline Ligands. *Cryst Growth Des* 13: 186-194.
 - Chen C, Bai FY, Zhang R, Song G, Shan H, et al. (2013) Synthesis, structure, and catalytic bromination of supramolecular oxovanadium complexes containing oxalate. *J Coord Chem* 66: 671-688.
 - Liang XL, Tan LF, Zhu WG (2011) Study on DNA-binding and DNA-cleavage properties of Cr(III) complexes with polypyridyl ligands. *DNA Cell Biol* 30: 61-67.
 - Li H, Bo H, Wang J, Shao H, Huang S (2011) Separation of supercoiled from open circular forms of plasmid DNA, and biological activity detection. *Cytotechnology* 63: 7-12.